

## Supporting Information

### Polypyrrole/NiFe-Layered double hydroxide composite as an anticorrosive microwave absorber

Haoxiang Zhai<sup>a</sup>, Lihong Wu<sup>a,b,c</sup>, Lei Yu<sup>a,b,c</sup>, Liang Li<sup>a,b</sup>, Gengping Wan<sup>a,b,c\*</sup>,  
Ying Zhang<sup>a</sup>, Xiang Yuan<sup>a</sup>, Jieping Wang<sup>a</sup>, Guizhen Wang<sup>a,b,c\*</sup>

<sup>a</sup> *Center for Advanced Studies in Precision Instruments, School of Material Science and Engineering, Hainan University, Haikou 570228 Hainan, China.*

<sup>b</sup> *Key Laboratory of Pico Electron Microscopy of Hainan Province, Hainan University, Haikou, Hainan 570228, China.*

<sup>c</sup> *Center for New Pharmaceutical Development and Testing of Haikou, Haikou, Hainan 570228, China*

\* Corresponding authors.

E-mail addresses: wanggengping001@163.com (Gengping Wan);  
wangguizhen@hainanu.edu.cn (Guizhen Wan)

## 1. Experimental section

### 1.1 Materials

$\text{Fe}(\text{NO}_3)_3 \cdot 9\text{H}_2\text{O}$ ,  $\text{NH}_4\text{F}$ ,  $\text{NaNO}_3$ , and  $\text{CH}_4\text{N}_2\text{O}$  were purchased from Shanghai Macklin Biochemical Technology Co., Ltd. Ethyl alcohol, HCl, and acetone, were purchased from XiLong Science Co., Ltd. PPy and  $\text{Ni}(\text{NO}_3)_2 \cdot 6\text{H}_2\text{O}$  were purchased from Shanghai Aladdin Biochemical Technology Co., Ltd. Nickel foam was purchased from Changde Liyuan New Material Co., Ltd. All the reagents were analytical grade and used without further purification.

### 1.2 Preparation of NiFe-LDH

To obtain NiFe-LDH, nickel foam should be pre-treated to remove oil and oxide layers. The nickel foam was cut into  $2 \times 2$  cm pieces and sonicated in 3 M HCl for 20 min, followed by washing with acetone and anhydrous ethanol and vacuum drying. NiFe-LDH was synthesized by the hydrothermal method. 0.0012 mol of  $\text{Ni}(\text{NO}_3)_2 \cdot 6\text{H}_2\text{O}$ , 0.0010 mol of  $\text{Fe}(\text{NO}_3)_3 \cdot 9\text{H}_2\text{O}$ , and 0.0028 mol of  $\text{CH}_4\text{N}_2\text{O}$  were dissolved in 100 mL water, stirred for 20 min, and then 0.7408 g  $\text{NH}_4\text{F}$  was added and stirred for 15 min. 80 mL of the prepared solution was transferred to a 100 mL reaction vessel, and the nickel foam was added. The reaction was carried out at  $150^\circ\text{C}$  for 48 h. The obtained sample was washed with deionized water and vacuum dried at  $60^\circ\text{C}$  for 24 h.

### 1.3 Preparation of PPy@NiFe-LDH

PPy was deposited on NiFe-LDH through electrodeposition. A three-electrode system was used with the sample from the previous step as the working electrode, platinum and Ag/AgCl as the counter and reference electrodes, respectively. The electrode was immersed in 0.2 M  $\text{NaNO}_3$  solution and 200  $\mu\text{L}$  pyrrole electrolyte, and electrodeposition was carried out at a voltage of 0.70 V for 25–55 min. The deposited samples were collected, washed with deionized water, and vacuum dried at  $60^\circ\text{C}$  for 24 h. Finally, the prepared PPy@NiFe-LDH samples were scraped from the nickel foam to study their MA properties.

## 2. Characterization

The morphology was analyzed by field emission scanning electronic microscopy (FESEM, Verios G4 UC) and energy dispersive spectroscopy (EDS). Transmission electron microscopy (TEM) was collected by using the transmission electron microscopy system (Thermo Scientific, Talos F200X G2). The phase and crystal structure were determined by X-ray diffraction (XRD, Smart Lab II, Cu K $\alpha$  radiation) and Raman spectrometry (Renishaw inVia Reflex, 514 nm laser). The surface chemical compositions were analyzed by X-ray photoelectron spectroscopy (XPS, AXIS SUPRA, Al K $\alpha$  source). (Bruker Tensor27) was employed to measure the Fourier transform infrared (FTIR) spectra. The electromagnetic parameters of the PPy@NiFe-LDH over a frequency range of 2.00–18.00 GHz were tested using the coaxial wire method with a vector network analyzer (Agilent N5230A). PPy@NiFe-LDH (10 wt%) were mixed with paraffin and then reshaped into a coaxial ring with an outer diameter of 7.00 mm, an inner diameter of 3.04 mm and a thickness of 2.00 mm. Investigations on microwave absorption properties and mechanism analysis were deduced according to the electromagnetic parameters. The involved equations are explained in detail in the Supporting Information.

Potentiodynamic polarization curve, electrochemical impedance spectroscopy (EIS), and open circuit potential (OCP) were determined by CHI660E electrochemical workstation through a three-electrode system at room temperature including a reference electrode (saturated calomel electrode), a counter electrode (platinum foil) and a working electrode. The corrosion resistance of 35-PPy@NiFe-LDH was evaluated under different acidic, neutral and alkaline non-degassing static NaCl aqueous solutions (5 wt%) under extremely humid conditions. Besides, carbon steel (Q235) is placed in same solution. In the case of preparing the working electrode, the working electrode was prepared by dropping a mixed solution (12  $\mu\text{L}$ , 2 mg  $\mu\text{L}^{-1}$ ) on a glass carbon electrode with a diameter of 3.00 mm. The mixed solution was composed of 35-PPy@NiFe-LDH (5 mg), Nafion solution (6  $\mu\text{L}$ , 5 wt%) and ethanol (300  $\mu\text{L}$ ), and was treated with ultrasound for 20 min. To obtain electrochemical stability, the OCP test lasted about 40 min. The EIS measurement was measured with the perturbed potential of 10.0 mV in the frequency range from  $10^{-2}$  to  $10^5$  Hz. The EIS data were modeled and fitted by equivalent circuit model and ZSimpWin software, respectively. The OCP with

a potentiodynamic polarization curve scanning rate of 1 mV s<sup>-1</sup> was measured in the voltage range of -0.8 V to 0.4 V.

### 3. Electromagnetic formula

The reflection loss values of as-prepared samples were researched according to the transmission line theory:

$$Z_{in} = Z_0 \sqrt{\mu_r / \varepsilon_r} \tan h(j2\pi f d / c \sqrt{\mu_r \varepsilon_r}) \quad (\text{Eq. S1})$$

$$RL = 20 \log |(Z_{in} - Z_0) / Z_{in} + Z_0| \quad (\text{Eq. S2})$$

where  $Z_{in}$  is the input impedance of the absorber,  $Z_0$  is the impedance of free space,  $\mu_r$  is the relative complex permeability,  $\varepsilon_r$  is the complex permittivity,  $f$  is the frequency of microwaves,  $c$  is the velocity of light, and  $d$  is the thickness of the absorber.

The impedance matching can be expressed as the equation:

$$Z = Z_{in} / Z_0 = \sqrt{|\mu_r / \varepsilon_r|} \tan h[j(2\pi f d / c) \sqrt{\mu_r \varepsilon_r}] \# \quad (\text{Eq. S3})$$

where  $Z_{in}$  is the impedance of the microwave absorber and  $Z_0$  is the impedance of free space. When the  $Z$  value is close to 1, the microwave can enter into the absorber easily and then be converted to thermal or other energy.

The complex permittivity and permeability can be expressed as the equation:

$$\varepsilon_r = \varepsilon' - j\varepsilon'' \# \quad (\text{Eq. S4})$$

$$\mu_r = \mu' - j\mu'' \# \quad (\text{Eq. S5})$$

$\varepsilon'$  and  $\mu'$  are related to the storage capacity of electromagnetic energy, while  $\varepsilon''$  and  $\mu''$  are related to energy dissipation and magnetic loss.

$\alpha$  can be expressed as the equation:

$$\alpha = \sqrt{2\pi f / c} \sqrt{(\mu'' \varepsilon'' - \mu' \varepsilon') + \sqrt{(\mu'' \varepsilon'' - \mu' \varepsilon')^2 + (\mu' \varepsilon'' + \mu'' \varepsilon')^2}} \quad (\text{Eq. S6})$$

In the formula,  $\varepsilon_s$  and  $\varepsilon_\infty$  mean the static permittivity and relative permittivity at the high frequency limit, respectively.

$$t_m = nc / (4f_m \sqrt{|\mu_r| |\varepsilon_r|}) (n = 1, 3, 5 \dots) \# \quad (\text{Eq. S7})$$

where  $|\mu_r|$  and  $|\varepsilon_r|$  are the modulus of the  $\mu_r$  and  $\varepsilon_r$ , respectively.

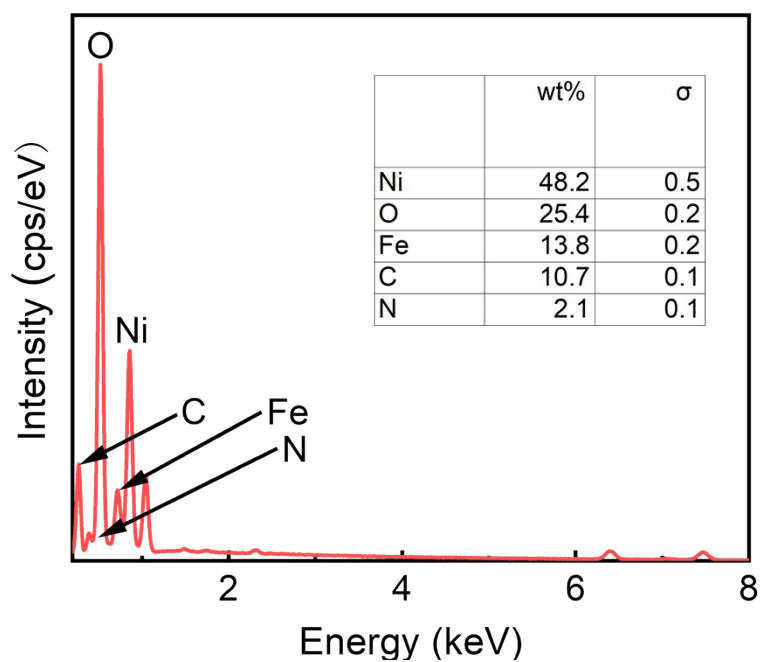


Fig. S1 EDS energy spectrum of the 35-PPy@NiFe-LDH.

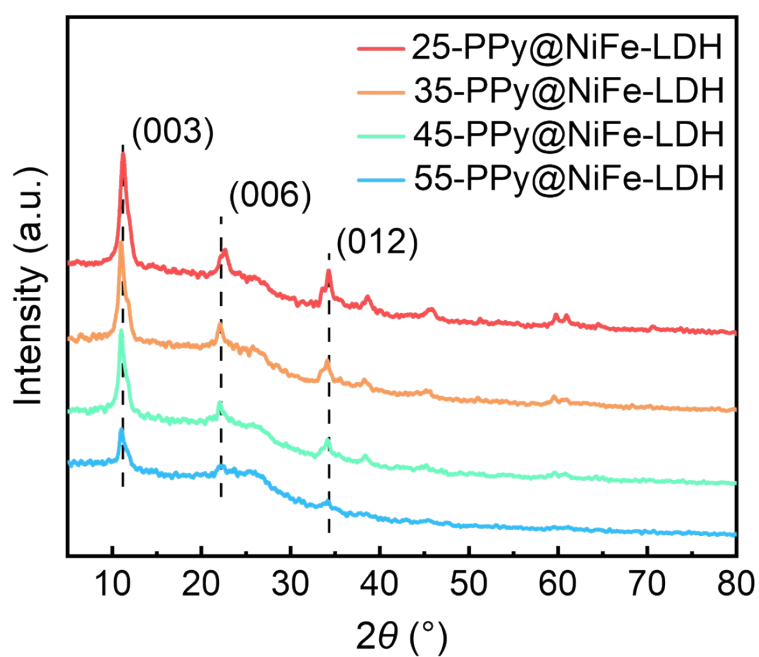


Fig. S2 XRD of PPy@NiFe-LDH under different deposition time.

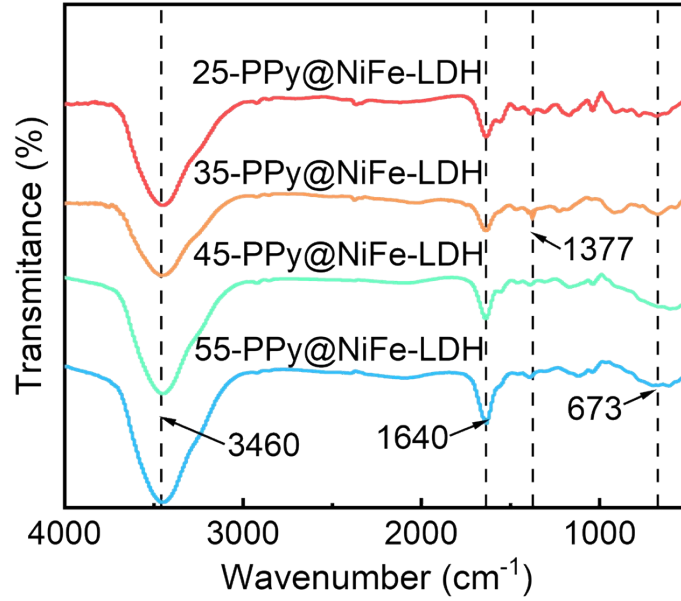


Fig. S3 FTIR spectra of PPy@NiFe-LDH under different deposition time.

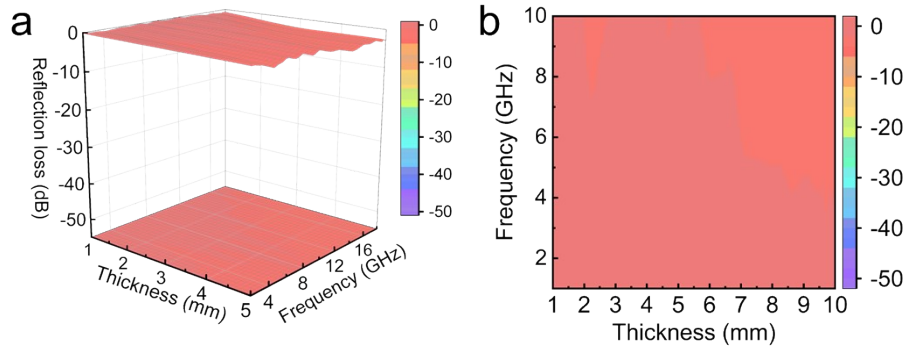


Fig. S4 (a) 3D RL values and (b) corresponding projection plots of NiFe-LDH.

Table S1 The comparison of MA properties of various absorbing materials.

| Materials                               | RL <sub>min</sub> | Thickness     | EAB <sub>max</sub> | Thickness     | Filling amount (wt%) |
|---|-------------------|---------------|--------------------|---------------|----------------------|
| NiAl-LDH/G                              | -41.5 dB          | 1.4 mm        | 4.40 GHz           | 1.6 mm        | 7                    |
| C/NiFe-LDH                              | -51.8 dB          | 3.5 mm        | 4.00 GHz           | 2.0 mm        | 15                   |
| MnO <sub>2</sub> @ZnCoNi-LDH            | -56.3 dB          | 2.4 mm        | 4.56 GHz           | 2.1 mm        | Not given            |
| FeNi@C                                  | -30.4 dB          | 1.2 mm        | 4.60 GHz           | 1.4 mm        | 33                   |
| Ni@Co/C@PPy                             | -48.7 dB          | 2.0 mm        | 5.54 GHz           | 2.2 mm        | 40                   |
| C/Ni/PPy                                | -42.1 dB          | 2.4 mm        | 5.24 GHz           | 2.5 mm        | 30                   |
| PPy/Ni/RGO                              | -47.3 dB          | 4.0 mm        | 4.32 GHz           | 1.5 mm        | 30                   |
| GNS-Fe <sub>3</sub> O <sub>4</sub> @PPy | -49.3 dB          | 2.0 mm        | 4.08 GHz           | 1.5 mm        | 30                   |
| <b>This work (PPy@NiFe-LDH)</b>         | <b>-59.5 dB</b>   | <b>3.8 mm</b> | <b>6.08 GHz</b>    | <b>2.4 mm</b> | <b>10</b>            |

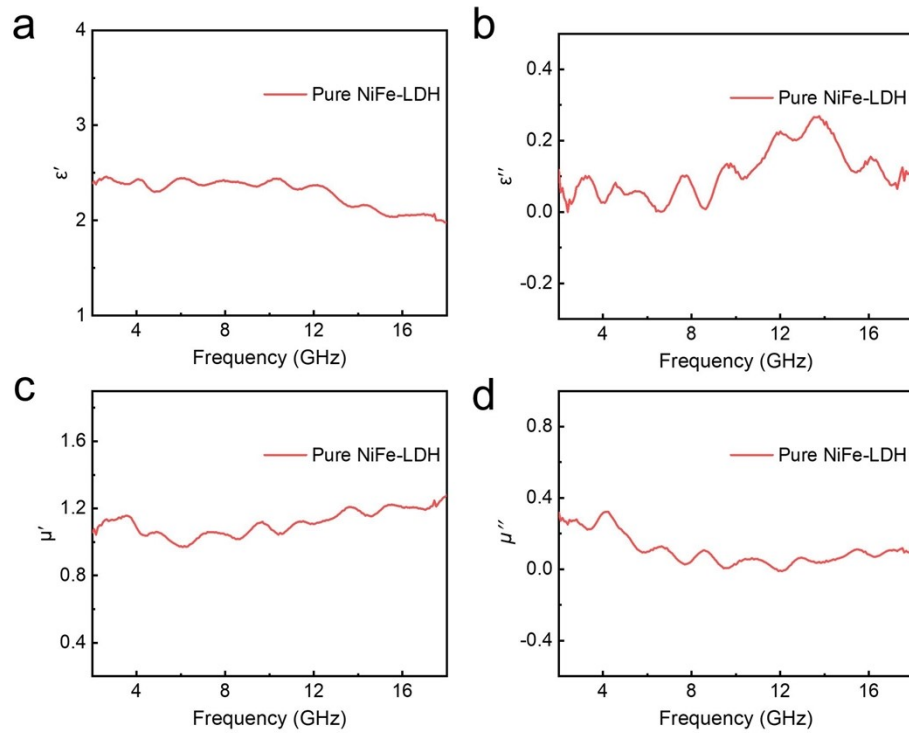


Fig. S5 (a)  $\epsilon'$ , (b)  $\epsilon''$ , (c)  $\mu'$ , and (d)  $\mu''$  curves of NiFe-LDH.

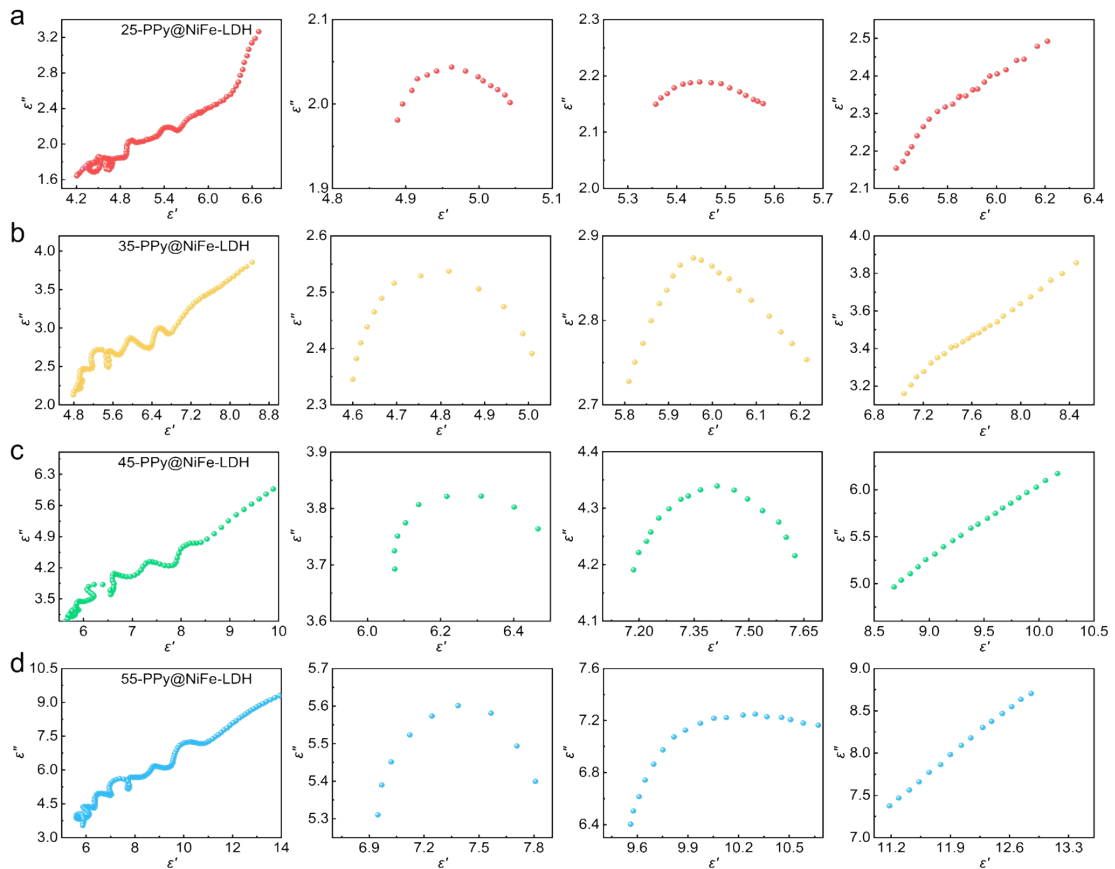


Fig. S6 Cole-Cole plots of PPY@NiFe-LDH under different deposition time.

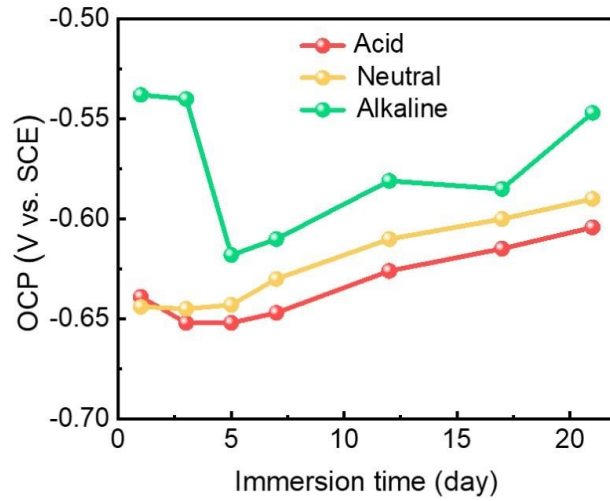


Fig. S7 Evolution of OCP values of Q235 in different pH salt solutions.

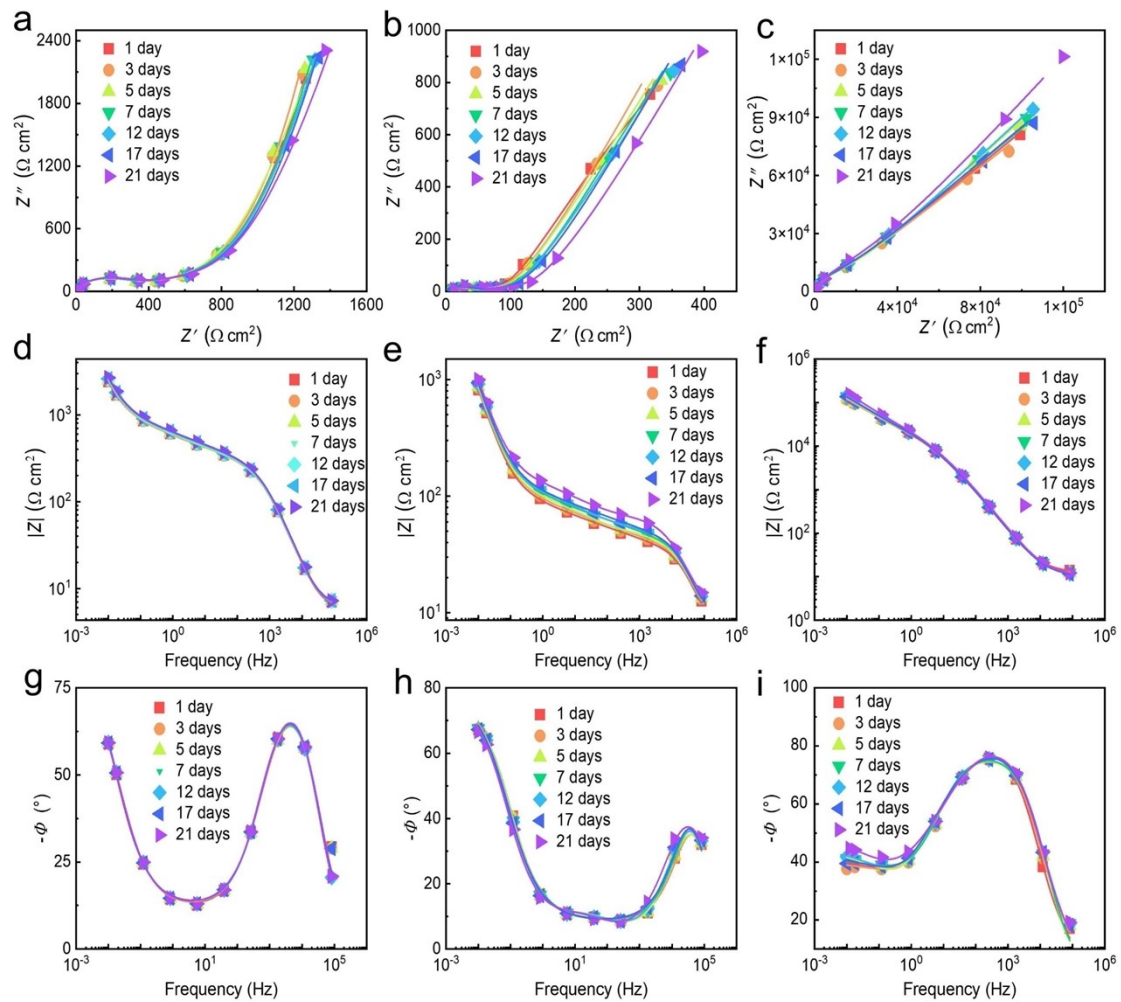


Fig. S8 Nyquist plots, Bode plots, and phase angle plots of (a, d, g) acidic solution, (b, e, h) neutral solution, (c, f, i) alkaline solution.



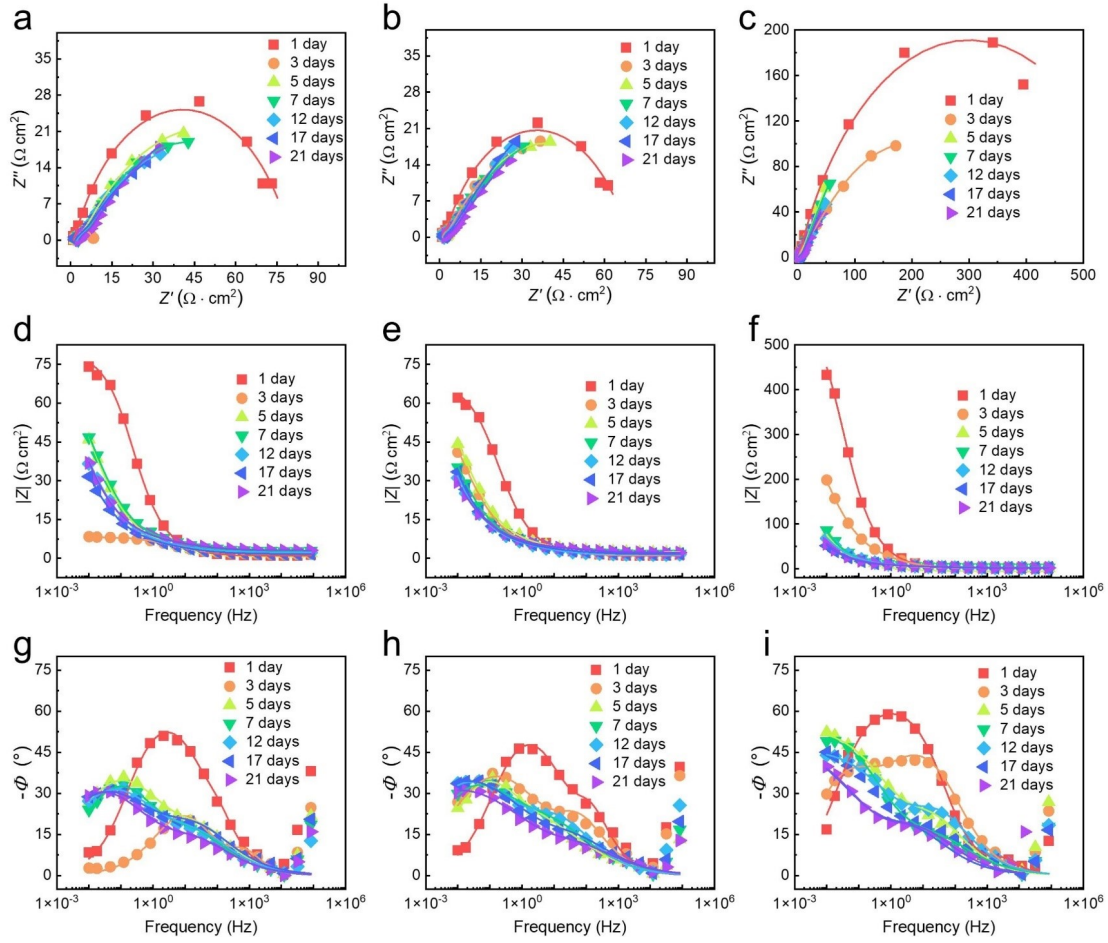


Fig. S9 Nyquist plots, Bode plots, and phase angle plots of (a, d, g) acidic solution, (b, e, h) neutral solution, and (c, f, i) alkaline solution of Q235.

Table S2 Corrosion kinetic parameters of 35-PPy@NiFe-LDH immersed in acidic, neutral, and alkaline solutions for 21 days, respectively.

| Solution | $E_{corr}$ [V] | $I_{corr}$ [ $A \cdot cm^{-2}$ ] | $\beta_a$ [mV] | $\beta_c$ [mV] | $R_p$ [ $\Omega$ ] |
|----------|----------------|----------------------------------|----------------|----------------|--------------------|
| Acid     | -0.250         | 2.431E-06                        | 2.758          | 3.979          | 2.655E+04          |
| Neutral  | -0.243         | 2.461E-06                        | 6.278          | 4.043          | 1.712E+04          |
| Alkaline | -0.243         | 1.742E-06                        | 5.909          | 3.952          | 2.531E+04          |

$$R_p = \beta_a \beta_c / I_{corr} \ln(10) (\beta_a + \beta_c) \quad (\text{Eq. S8})$$

Here,  $\beta_a$  and  $\beta_c$  are on behalf of the slopes of anodic and cathodic Tafel plots, respectively. It can be concluded from Table S1 that the value of  $I_{corr}$  is in the following order:  $I_{corr}\text{-alkaline} < I_{corr}\text{-acid} < I_{corr}\text{-neutral}$ , for  $R_p$ ,  $R_p\text{-acid}$  is the largest and  $R_p\text{-neutral}$  is the smallest. In general,  $I_{corr}$  and  $R_p$  can be used as parameters for qualitatively judging the anti-corrosion property of the coating, the smaller the value of  $I_{corr}$ , the

better anti-corrosion property of the coating while for  $R_p$ , the larger, the better. Hence, it can be preliminarily judged that the anti-corrosion property of the coating immersed in alkaline solution was the best, for that of the coating immersed in acidic solution the second and for that of the coating immersed in neutral solution the worst.

Table S3 Equivalent circuit of the samples immersed in acidic, neutral, and alkaline solutions after 21 days, respectively.

| Acidic: R(Q(QR(QR)))W   |          |          |          |          |           |          |           |
|---|----------|----------|----------|----------|-----------|----------|-----------|
| Acidic  | 1 day    | 3 days   | 5 days   | 7 days   | 12 days   | 17 days  | 21 days   |
| <b>R (<math>\Omega \text{ cm}^2</math>)</b>                   | 6.24     | 6.24     | 6.44     | 6.12     | 6.09      | 6.17     | 5.44      |
| <b>CPE-<math>Y_0</math> (<math>\text{F cm}^{-2}</math>)</b>   | 2.00E-06 | 2.00E-06 | 1.93E-06 | 2.02E-06 | 2.02E-06  | 1.99E-06 | 2.33E-06  |
| <b>n</b>  | 8.00E-01 | 9.24E-01 | 9.28E-01 | 9.27E-01 | 9.27E-01  | 9.27E-01 | 9.25E-01  |
| <b>CPE-<math>Y_0</math> (<math>\text{Fcm}^{-2}</math>)</b>    | 6.92E-03 | 1.38E-03 | 1.39E-03 | 9.74E-03 | 9.68E-03  | 1.46E-03 | 4.31E-03  |
| <b>n</b>  | 8.00E-01 | 8.00E-01 | 1.55E-01 | 9.90E-01 | 9.99E-01  | 8.00E-01 | 8.00E-01  |
| <b>R (<math>\Omega \text{ cm}^{-2}</math>)</b>                | 7.12E+01 | 7.12E+01 | 5.85E+01 | 1.21E+02 | 8.89E+01  | 4.07E-03 | 1.53E-02  |
| <b>CPE-<math>Y_0</math> (<math>\text{F cm}^{-2}</math>)</b>   | 1.38E-03 | 6.92E-03 | 6.85E-03 | 8.54E-04 | 1.00E-03  | 8.99E-03 | 1.09E-03  |
| <b>n</b>  | 8.00E-01 | 8.00E-01 | 9.42E-01 | 2.44E-01 | 2.04E-01  | 8.00E-01 | 6.97E-01  |
| <b><math>R_{ct}</math> (<math>\Omega \text{ cm}^2</math>)</b> | 2.17E+02 | 1.48E+02 | 7.14E+01 | 8.95E+01 | 1.24E+02  | 6.38E+01 | 6.80E+01  |
| <b>Warburg (<math>\Omega \text{ cm}^{-2}</math>)</b>          | 1.00E-03 | 1.77E-03 | 1.76E-03 | 5.42E-03 | 6.32E-03  | 1.10E-02 | 2.04E-03  |
| Neutral: R(Q(QR(QR)))W  |          |          |          |          |           |          |           |
| Neutral   | 1 day    | 3 days   | 5 days   | 7 days   | 12 days   | 17 days  | 21 days   |
| <b>R (<math>\Omega \text{ cm}^2</math>)</b>                   | 8.00     | 8.18     | 7.86     | 7.64     | 7.54      | 7.57     | 7.49      |
| <b>CPE-<math>Y_0</math> (<math>\text{F cm}^{-2}</math>)</b>   | 2.96E-07 | 2.54E-07 | 1.88E-07 | 2.11E-07 | 1.91E-07  | 1.80E-07 | 1.49E-07  |
| <b>n</b>  | 2.20E-01 | 2.24E-01 | 2.32E-01 | 2.29E-01 | 2.32E-01  | 2.34E-01 | 2.39E-01  |
| <b>CPE-<math>Y_0</math> (<math>\text{F cm}^{-2}</math>)</b>   | 1.15E-03 | 1.12E-03 | 9.13E-04 | 1.17E-03 | 1.13E-03  | 1.13E-03 | 1.08E-03  |
| <b>n</b>  | 2.52E-01 | 2.50E-01 | 2.35E-01 | 2.48E-01 | 2.44E-01  | 2.42E-01 | 2.38E-01  |
| <b>R (<math>\Omega \text{ cm}^2</math>)</b>                   | 5.70E+01 | 5.46E+01 | 4.10E+01 | 4.06E+01 | 3.68E+01  | 3.49E+01 | 3.20E+01  |
| <b>CPE-<math>Y_0</math> (<math>\text{F cm}^{-2}</math>)</b>   | 1.96E-06 | 2.04E-04 | 2.53E-04 | 2.12E-02 | 2.28E-04  | 2.36E-06 | 2.61E-04  |
| <b>n</b>  | 2.26E-01 | 2.26E-01 | 2.26E-01 | 2.26E-01 | 2.26E-01  | 2.26E-01 | 2.26E-01  |
| <b><math>R_{ct}</math> (<math>\Omega \text{ cm}^2</math>)</b> | 6.54E+01 | 6.92E+01 | 7.78E+01 | 5.77E+01 | 5.71E+01  | 5.65E+01 | 5.81E+01  |
| <b>Warburg (<math>\Omega \text{ cm}^{-2}</math>)</b>          | 1.92E-03 | 2.11E-03 | 5.13E+15 | 2.83E-03 | 3.88E-03  | 4.55E-03 | 9.86E-05  |
| Alkaline: R(Q(QR(QR)))W                                       |          |          |          |          |           |          |           |
| Alkaline  | 1 day    | 3 days   | 5 days   | 7 days   | 12 days   | 17 days  | 21 days   |
| <b>R (<math>\Omega \text{ cm}^2</math>)</b>                   | 9.67     | 9.48     | 9.03     | 9.21     | 9.28      | 11.50    | 9.57      |
| <b>CPE-<math>Y_0</math> (<math>\text{F cm}^{-2}</math>)</b>   | 1.48E-06 | 1.46E-06 | 1.54E-06 | 1.53E-06 | 1.24E-07  | 4.10E-06 | 1.64E-06  |
| <b>n</b>  | 8.34E-01 | 8.31E-01 | 8.85E-01 | 9.20E-01 | 2.82 E-01 | 8.70E-01 | 8.56 E-01 |
| <b>CPE-<math>Y_0</math> (<math>\text{Fcm}^{-2}</math>)</b>    | 2.99E-05 | 2.99E-05 | 3.03E-05 | 3.26E-05 | 2.65E-06  | 3.11E-05 | 3.19E-05  |
| <b>n</b>  | 5.32E-01 | 5.44E-01 | 4.70E-01 | 5.05E-01 | 1.39 E-01 | 4.90E-01 | 4.45E-01  |
| <b>R (<math>\Omega \text{ cm}^2</math>)</b>                   | 8.67E+02 | 8.50E+02 | 3.72E+02 | 6.09E+02 | 6.24E+02  | 1.17E+04 | 7.02 E+03 |
| <b>CPE-<math>Y_0</math> (<math>\text{F cm}^{-2}</math>)</b>   | 2.48E-05 | 2.20E-07 | 1.89E-05 | 1.85E-07 | 1.53E-06  | 2.92E-05 | 2.07E-05  |
| <b>n</b>  | 8.00E-01 | 8.00E-01 | 8.00E-01 | 8.00E-01 | 8.00 E-01 | 8.00E-01 | 8.00 E-01 |
| <b><math>R_{ct}</math> (<math>\Omega \text{ cm}^2</math>)</b> | 3.06E+04 | 2.64E+04 | 2.37E+04 | 2.03E+04 | 2.64E+04  | 1.90E+04 | 1.53E+04  |
| <b>Warburg (<math>\Omega \text{ cm}^{-2}</math>)</b>          | 4.32E-04 | 4.46E-04 | 4.83E-04 | 4.66E-04 | 3.67E-05  | 5.50E-05 | 4.53E-08  |

Table S4 Equivalent circuit of the Q235 immersed in acidic, neutral, and alkaline solutions after 21 days, respectively.

| Acidic: R(QR)(QR)                 |        |        |        |        |         |         |         |
|-----------------------------------|--------|--------|--------|--------|---------|---------|---------|
| Acidic (Q235)                     | 1 day  | 3 days | 5 days | 7 day  | 12 days | 17 days | 21 days |
| R ( $\Omega \text{ cm}^2$ )       | 1.08   | 1.60   | 1.89   | 2.80   | 2.15    | 1.67    | 1.67    |
| CPE- $Y_0$ ( $\text{F cm}^{-2}$ ) | 0.01   | 0.01   | 0.07   | 0.02   | 0.09    | 0.11    | 0.11    |
| n                                 | 0.92   | 1.00   | 0.56   | 0.58   | 0.54    | 0.51    | 0.51    |
| R ( $\Omega \text{ cm}^{-2}$ )    | 0.34   | 0.35   | 93.40  | 3.17   | 82.50   | 885.00  | 885.00  |
| CPE- $Y_0$ ( $\text{Fcm}^{-2}$ )  | 0.01   | 0.03   | 0.03   | 0.07   | 0.04    | 0.04    | 0.04    |
| n                                 | 0.73   | 0.64   | 0.62   | 0.59   | 0.53    | 0.54    | 0.54    |
| R ( $\Omega \text{ cm}^{-2}$ )    | 78.70  | 6.36   | 20.20  | 75.60  | 2.63    | 2.94    | 2.94    |
| Neutral: R(QR)(QR)                |        |        |        |        |         |         |         |
| Neutral (Q235)                    | 1 day  | 3 days | 5 days | 7 day  | 12 days | 17 days | 21 days |
| R ( $\Omega \text{ cm}^2$ )       | 1.04   | 1.18   | 2.25   | 1.74   | 1.43    | 1.65    | 2.20    |
| CPE- $Y_0$ ( $\text{F cm}^{-2}$ ) | 0.00   | 0.01   | 0.06   | 0.11   | 0.12    | 0.11    | 0.12    |
| n                                 | 0.89   | 0.73   | 0.45   | 0.55   | 0.53    | 0.49    | 0.44    |
| R ( $\Omega \text{ cm}^{-2}$ )    | 0.89   | 1.53   | 4.99   | 83.52  | 116.00  | 184.40  | 215.00  |
| CPE- $Y_0$ ( $\text{F cm}^{-2}$ ) | 0.02   | 0.07   | 0.08   | 0.07   | 0.05    | 0.05    | 0.04    |
| n                                 | 0.71   | 0.56   | 0.64   | 0.49   | 0.58    | 0.51    | 0.52    |
| R ( $\Omega \text{ cm}^{-2}$ )    | 66.75  | 77.64  | 64.74  | 3.63   | 2.68    | 18.74   | 15.38   |
| Alkaline: R(QR)(QR)               |        |        |        |        |         |         |         |
| Alkaline (Q235)                   | 1 day  | 3 days | 5 days | 7 day  | 12 days | 17 days | 21 days |
| R ( $\Omega \text{ cm}^2$ )       | 2.02   | 1.68   | 1.61   | 2.78   | 1.62    | 2074.00 | 2.02    |
| CPE- $Y_0$ ( $\text{F cm}^{-2}$ ) | 0.01   | 0.01   | 0.07   | 0.07   | 0.02    | 0.09    | 0.02    |
| n                                 | 0.73   | 0.64   | 0.61   | 0.63   | 0.61    | 0.55    | 0.53    |
| R ( $\Omega \text{ cm}^{-2}$ )    | 596.00 | 219.40 | 244.40 | 118.10 | 339.40  | 127.20  | 367.90  |
| CPE- $Y_0$ ( $\text{F cm}^{-2}$ ) | 0.00   | 0.02   | 0.03   | 0.03   | 0.07    | 0.03    | 0.08    |
| n                                 | 1.00   | 0.64   | 0.59   | 0.55   | 0.53    | 0.53    | 0.54    |
| R ( $\Omega \text{ cm}^{-2}$ )    | 0.32   | 33.63  | 2.96   | 3.39   | 33.34   | 35.96   | 25.39   |

$R_{ct}$  is the resistance of the coating.  $Q_{dl}$  and  $R_{ct}$  represent the constant phase angle element of the electric double layer, and the charge transfer resistance, that is, the interface resistance between the electrolyte solution and the substrate.